

The adipose organ of obesity-prone C57BL/6J mice is composed of mixed white and brown adipocytes[§]

A. Vitali,* I. Murano,* M.C. Zingaretti,* A. Frontini,* D. Ricquier,[†] and S. Cinti^{1,*§}

Department of Experimental and Clinical Medicine,* University of Ancona (Politecnica delle Marche), 60020 Ancona, Italy; Université Paris Descartes,[†] CNRS and INSERM Cochin Institute, Paris, France; and The Adipose Organ Lab,[§] IRCCS San Raffaele Pisana, 00163 Rome, Italy

Abstract White and brown adipocytes are believed to occupy different sites in the body. We studied the anatomical features and quantitative histology of the fat depots in obesity and type 2 diabetes-prone C57BL/6J mice acclimated to warm or cold temperatures. Most of the fat tissue was contained in depots with discrete anatomical features, and most depots contained both white and brown adipocytes. Quantitative analysis showed that cold acclimation induced an increase in brown adipocytes and an almost equal reduction in white adipocytes; however, there were no significant differences in total adipocyte count or any signs of apoptosis or mitosis, in line with the hypothesis of the direct transformation of white into brown adipocytes. The brown adipocyte increase was accompanied by enhanced density of noradrenergic parenchymal nerve fibers, with a significant correlation between the density of these fibers and the number of brown adipocytes. Comparison with data from obesity-resistant Sv129 mice disclosed a significantly different brown adipocyte content in C57BL/6J mice, suggesting that this feature could underpin the propensity of the latter strain to develop obesity. However, the greater C57BL/6J browning capacity can hopefully be harnessed to curb obesity and type 2 diabetes in patients with constitutively low amounts of brown adipose tissue.—Vitali, A., I. Murano, M. C. Zingaretti, A. Frontini, D. Ricquier, and S. Cinti. **The adipose organ of obesity-prone C57BL/6J mice is composed of mixed white and brown adipocytes.** *J. Lipid Res.* 2012. 53: 619–629.

Supplementary key words adipose tissue • beta-oxidation • diabetes • innervations • transdifferentiation

All mammals are provided with the chemical energy-storing white adipose tissue (WAT) and the energy-dissipating brown adipose tissue (BAT) (1–3).

BAT, which is generally considered as being composed of multilocular adipocytes immunoreactive for uncoupling protein1 (UCP1), its functional thermogenic protein, and WAT, a tissue widely believed to be composed of UCP1-negative unilocular adipocytes, are commonly held

to occupy distinct anatomical sites in the body. However, previous work, mainly from our lab, supports the notion that WAT and BAT are in fact found together in subcutaneous and visceral fat depots, collectively forming a multi-depot organ that we have called the “adipose organ” (4, 5). This finding has opened new perspectives in the physiological relationship between BAT and WAT, including the possibility of their reciprocal transformation (transdifferentiation) (6–8). Harnessing the mechanism of WAT to BAT transdifferentiation could be useful to develop treatments for obesity and type 2 diabetes, because the absence of BAT or its β adrenergic receptors results in obesity (9, 10) and transgenic mice overexpressing UCP1 in WAT are obesity resistant (11). Furthermore, treatment of obese rodents with β 3 agonists increases BAT and curbs obesity (12, 13). Recently, metabolically active BAT has been described in adult humans. Of note, these subjects have a lower body mass index (BMI) and less visceral fat than those without detectable BAT (14–20). C57BL/6J mice are obesity- and type 2 diabetes-prone (21). In fact, earlier work has shown that C57BL/6J mice are more predisposed to store fat in response to a high-fat diet and to develop obesity, hyperglycemia, and hyperinsulinemia than their obesity-resistant A/J counterparts (22). Furthermore, it has been suggested that the obesity and diabetes resistance of A/J mice may be due to a strong increase in brown adipocytes in some “classic” white adipose depots after cold exposure or treatment with a β 3 adrenergic agonist (23, 24). Also, a previous work by our group showed that intermuscular fat in the hind legs of C57BL/6J mice contains fewer brown adipocytes than the intermuscular fat of obesity-resistant Sv129 mice (substrain 129/SVPAS SPF/VAF), suggesting the possibility that a difference in BAT amount could explain the susceptibility to obesity and type 2 diabetes of C57BL/6J

Abbreviations: ABC, avidin-biotin-peroxidase complex; BAT, brown adipose tissue; H and E, hematoxylin-eosin; SNS, sympathetic nervous system; TH, tyrosine hydroxylase; UCP1, uncoupling protein 1; WAT, white adipose tissue.

¹To whom correspondence should be addressed.

e-mail: cinti@univpm.it

[§]The online version of this article (available at <http://www.jlr.org>) contains supplementary data in the form of two figures and two tables.

This work was supported by Fondazione Cariverona Grant 2008 (to S.C.) and by grants from Università Politecnica delle Marche.

Manuscript received 19 July 2011 and in revised form 23 January 2012.

Published, JLR Papers in Press, January 23, 2012

DOI 10.1194/jlr.M018846

mice (25). As intermuscular fat depots account for a very small fraction of the body fat, we decided to measure the total amount of BAT in the major subcutaneous and visceral fat depots of C57BL/6J mice. We then compared it to the data obtained on obesity-resistant Sv129 mice by two previous works performed in our lab (26, 27) to see whether, after measuring most of the fat contained in the body, the difference between the strains was significant. Furthermore, understanding WAT-BAT plasticity in different depots could be important as a presupposition for the treatment of obesity by BAT-inducing drugs (28). BAT induction through cold exposure and acclimation is mainly regulated by the sympathetic nervous system (SNS) (1). In Sv129 mice, BAT activation after cold acclimation correlated with the density of noradrenergic parenchymal fibers (26) measured by immunohistochemistry using tyrosine hydroxylase (TH) enzyme, a widely used marker for this type of nerve fibers (29). We therefore examined TH-positive parenchymal fibers in the fat depots of C57BL/6J mice to establish whether such correlation is also found in this strain.

The results showed that although the adipose organs of C57BL/6J and Sv129 mice share a fairly similar anatomy, including the mixed composition of most subcutaneous and visceral depots, they contain different amounts of multilocular UCP1-positive adipocytes, which are lower in C57BL/6J than in Sv129 mice. A significant increase in

this population of cells and an equal decrease in unilocular UCP1-negative adipocytes noted after cold acclimation suggest the possibility that the experimental condition triggered white to brown adipocytes transdifferentiation. There was a positive correlation between the density of TH-positive parenchymal nerve fibers and the amount of brown adipocytes. Our findings lend further support to the concepts of a mixed composition of most mouse fat depots, of their plasticity, and of a possible role of the SNS in determining their phenotype; moreover, they suggest that the total amount of brown adipocytes forming BAT, genetically determined and located in the adipose organ, could account for susceptibility to obesity and diabetes.

MATERIALS AND METHODS

Animals

Two groups of five 12-week-old C57BL/6J female mice (Harlan, Udine, Italy) were kept at 28°C (warm-acclimated) or at 6°C (cold-acclimated) for 10 days. A warm acclimation temperature of 28°C, instead of the usual 20–25°C, was chosen to reduce adrenergic stimulation. Moreover, this temperature is close to the thermoneutral temperature for mice (~30–34°C) (30). Mice were housed individually with a 12 h light/dark cycle and free access to food and water. All animal procedures were in accordance with Italian Institutional and National Guidelines and were approved by the Animal Ethics Committee of Università

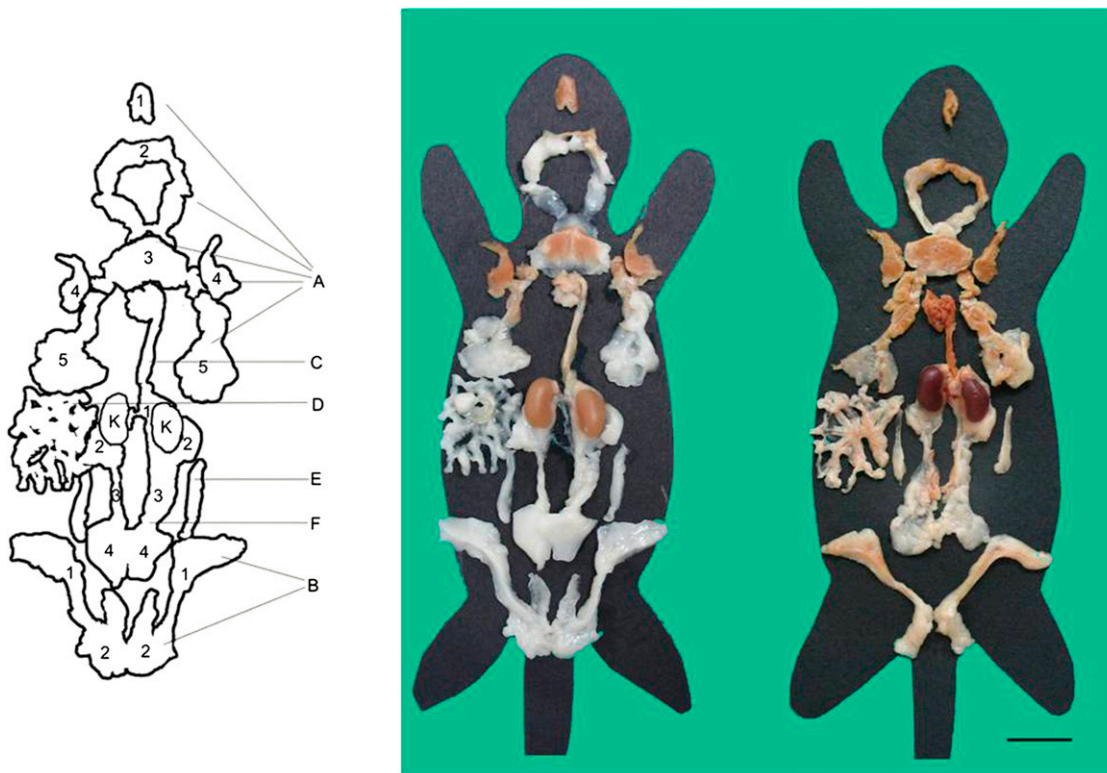


Fig. 1. Multi-depot adipose organ of adult C57BL/6J female mice kept at 28°C (left) or 6°C (right) for 10 days. Anatomical dissection under a surgical microscope. Each depot was placed on a mouse template indicating approximately its original anatomical position. Kidneys (K) were dissected together with the depots. The organ is made up of the two subcutaneous depots (A) anterior [1-deep cervical portion, 2-superficial cervical portion, 3-interscapular portion (interscapular BAT), 4-subscapular portion, 5-axillo-thoracic portion] and (B) posterior (1-inguinal-dorsolumbar portion, 2-gluteal portion), and the visceral depots (C) mediastinal (including the aortic arch and its thoracic portion), (D) mesenteric, (E) retroperitoneal, and (F) abdominopelvic (1-interrenal portion, 2-periovarian portion, 3-parametrial portion, 4-perivesical portion). Scale bar for both: 2 cm.

Politecnica delle Marche. Mice were euthanized with an overdose of anesthetic (ketamine) in combination with xylazine and immediately perfused transcardially with 4% paraformaldehyde in 0.1 M phosphate buffer, pH 7.4, for 3 min.

Tissue treatment

After perfusion, all visible fat depots of the adipose organ were anatomically dissected under a Zeiss OPII surgical microscope (Carl Zeiss, Germany). Each depot or part thereof was weighed and immersed in saline, and its volume was measured by fluid displacement. Afterward, all depots were fixed overnight in 4% paraformaldehyde at 4°C, dehydrated, cleared, and finally paraffin-embedded so that the cutting plane corresponded with the largest surface.

Light microscopy and immunohistochemistry

All depots were examined: anterior subcutaneous, posterior subcutaneous, mediastinal, mesenteric, abdominopelvic, and retroperitoneal.

The major fat depots were distinguished into subdepots as follows: anterior subcutaneous [interscapular (symmetric), subscapular (symmetric), axillo-thoracic (symmetric), superficial cervical (symmetric), deep cervical (symmetric)]; posterior subcutaneous [dorsolumbar-inguinal (symmetric), gluteal (symmetric)]; and visceral (abdominopelvic) [interrenal (symmetric), periovarian (symmetric), parametrial (symmetric), perivesical (symmetric)]. For reference, other nomenclatures for the fat depots are reported in supplementary Table I. Each paraffin-embedded depot or subdepot was cut at three different levels to ensure examination of a representative sample of its histological composition. Three serial sections per level (each 3 μm thick) were obtained and used for histological examination, morphometry [hematoxylin-eosin (H and E)], and immunohistochemistry (UCP1 and TH immunostaining), yielding a total of 66 sections per animal and 330 per condition. Each slide was examined at 400 \times final magnification for signs of apoptosis (31) or mitosis.

Serial sections were first stained for H and E, then used for immunohistochemical localization of UCP1 and TH proteins. UCP1 is a marker of brown adipocytes (1), and TH is a marker of adrenergic nerve fibers (29). One section was incubated with a polyclonal anti-rat UCP1 antibody raised in sheep (provided by D. Ricquier) at a final dilution of 1:3800 in PBS and the adjacent section with a rabbit anti-TH polyclonal antibody (Chemicon Millipore, Milan, Italy) at a final dilution of 1:700, according to the indirect avidin-biotin-peroxidase complex (ABC) method (32). The ability of the antibodies to detect the antigens specifically was assessed in sections of tissues known to contain the antigens (e.g., interscapular BAT of cold-acclimated mice and rats) (33, 34). Negative controls were obtained in each instance by omitting the primary antibody or replacing it with preimmune serum.

Morphometry

Adipocytes. The area of 500 unilocular and 500 multilocular adipocytes was measured in H and E sections of each subdepot using a digital image system (Lucia imaging, version 4.82, Praha, Czech Republic) to determine mean adipocyte volume, assuming that the cells had a spherical shape. In the same sections, we accurately traced the shape of all unilocular and multilocular adipocytes, interstitial spaces, and vascular and nerve structures and computed their respective areas. We then obtained the percentage space occupied by each type of structure and used these data to calculate the total percentage volume occupied by unilocular and multilocular adipocytes using the principle of Delesse, which

states that the percentage of the area fraction of a component is equal to its volume fraction (35). Finally, the absolute number of unilocular and multilocular adipocytes was obtained by dividing the total volume of unilocular and multilocular adipocytes by their mean volume.

The UCP1-immunostained sections of each depot were used to measure the percentage area occupied by UCP1-negative and UCP1-positive multilocular adipocytes. To do so, images of the total areas occupied by multilocular adipocytes were acquired by a digital light microscope (Nikon Eclipse 80i) at 200 \times final magnification. The areas were profiled manually using a digital image analysis system to calculate the percentage volume occupied by UCP1-positive and UCP1-negative multilocular adipocytes. Application of the principle of Delesse, mentioned above, and division of the total volume occupied by UCP1-negative and UCP1-positive multilocular adipocytes by their mean volume allowed calculation of the final absolute number of UCP1-positive and UCP1-negative multilocular adipocytes.

Sections stained for UCP1 were also used to count the number of lipid droplets and to measure their area in UCP1-positive and UCP1-negative multilocular adipocytes. Specifically, areas containing only UCP1-positive or only UCP1-negative multilocular adipocytes were selected at very low magnification (40 \times); they were then examined with automatic change of magnification (1000 \times) and automatically photographed with the Eclipse 80i digital light microscope, taking

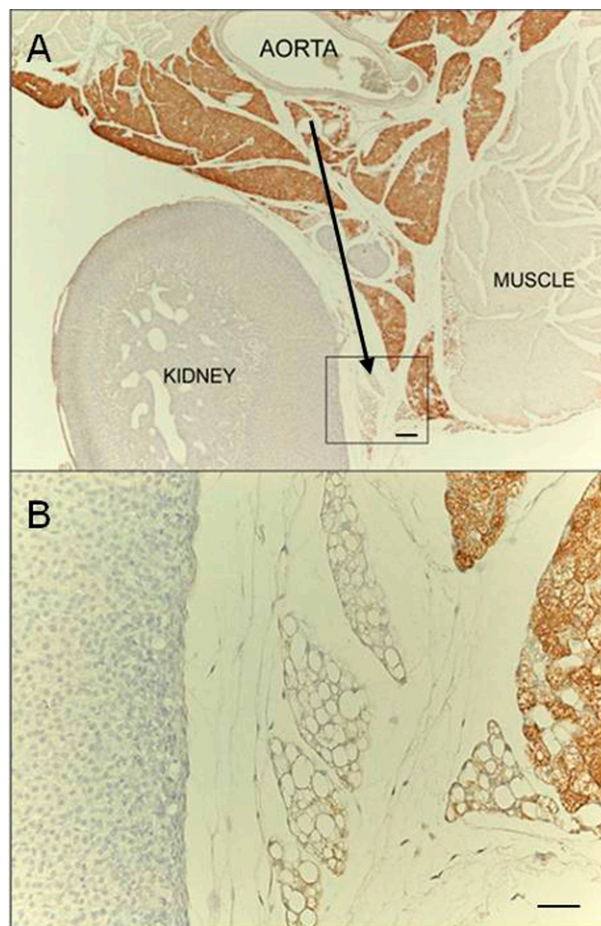


Fig. 2. UCP1 immunostaining. (A) Representative picture of interrenal fat showing that the tissue portion closest to the aorta is predominantly composed of UCP1-positive multilocular adipocytes, whereas the peripheral portion is predominantly composed of UCP1-negative unilocular adipocytes (black arrow). (B) Enlargement of framed area in A. Scale bar: 70 μm (A); 30 μm (B).

five photos/area. The photos were used to measure the number and area of lipid droplets in UCP1-positive and UCP1-negative multilocular adipocytes. An average of 60 adipocytes per subdepot (about 1,300 adipocytes/animal) was examined.

Parenchymal nerve fibers. Only parenchymal TH-positive fibers (i.e., those closely associated with adipocytes) were counted, whereas the perivascular TH-positive fibers were not considered.

Pure unilocular, multilocular and mixed adipocyte areas were selected at very low magnification (40×). Each area was studied by automatic change of magnification (1000×) and automatically photographed (Eclipse 80i microscope), taking 20 photos/area. The photos were used to measure the total number of cells and of TH-positive fibers. The final result was expressed as number of TH-positive fibers/100 adipocytes from 1,300 areas, which included all 14 subdepots from each mouse.

Statistical analysis

Results are given as mean ± SEM. Significance was analyzed using an unpaired *t*-test and a nonparametric test (Mann-Whitney test) (InStat, GraphPad, San Diego, CA). Differences between groups were considered significant when $P \leq 0.05$. Linear correlations were calculated by a nonparametric test (Spearman) using GraphPad Prism, version 4.01, for Windows.

RESULTS

Gross anatomy

Subcutaneous fat. The surgical microscope made it possible to isolate all the visible major fat depots that are found in the body of adult animals. We dissected the two main subcutaneous depots and several visceral depots. A connective capsule surrounded each depot, providing a cleavage plane and defining its anatomical border. The depots of animals kept at 28°C for 10 days (28°C mice) showed discrete anatomical features (shape and color) at all sites studied, both in the subcutaneous and in the visceral compartment (**Fig. 1**). Although depot shape and location were identical in both experimental conditions, their color was browner in animals kept at 6°C for 10 days (6°C mice). The two subcutaneous depots (see supplementary Table I for nomenclature) were located, respectively, in the anterior part of the body (anterior subcutaneous depot) adjacent to the origin of the fore limbs and in the posterior part of the body (posterior subcutaneous depot) adjacent to the origin of the hind limbs. Together, these two depots accounted for 53% (in 28°C mice)

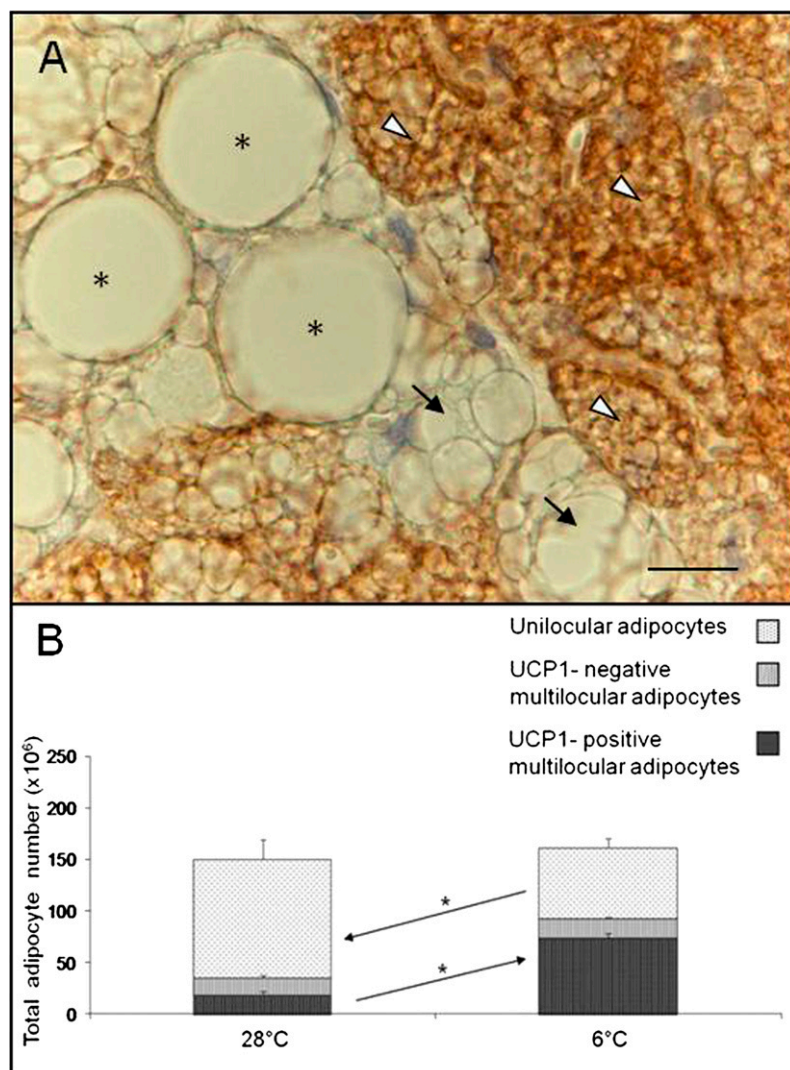


Fig. 3. (A) Interscapular BAT. UCP1 immunostaining of a C57BL/6J mouse maintained at 6°C for 10 days shows three different cell types: UCP1-negative unilocular adipocytes (*), UCP1-negative multilocular adipocytes (black arrows), and UCP1-positive multilocular adipocytes (white arrowheads). Scale bar: 10 μm. (B) Total number of adipocytes contained in the adipose organ of C57BL/6J mice maintained at 28°C or 6°C for 10 days. The overall number of adipocytes in the organ was not significantly changed in either experimental condition ($P = 0.14$). In the cold-acclimated group, the total number of UCP1-positive multilocular adipocytes increased significantly ($P = 0.01$). Unilocular adipocytes decreased significantly by the same amount ($P = 0.05$). UCP1-negative multilocular adipocytes were almost unchanged. Data are shown as mean ± SEM.

and 57% (in 6°C mice) of the volume of the whole adipose organ (the sum of all subcutaneous and visceral depots).

In 28°C mice, the anterior subcutaneous depot consisted of white and brown portions corresponding, on histology, to white and brown adipose tissue, respectively. The brown parts were predominantly located in the central portion of the depot (interscapular area) and in the symmetric subscapular, axillary, and deep cervical regions. The white parts were mainly located in the more peripheral symmetric extensions of the depot and in the superficial portion of the cervical region (Fig. 1).

In 6°C mice, the white parts of the depot had almost disappeared (Fig. 1), leaving a small number of white areas in the superficial cervical region and in the thoracic portion.

The posterior subcutaneous depot consisted of two long strands surrounding the basal portion of each hind limb, from the dorsolumbar region to the inguinal and gluteal parts, that were joined at the level of the pubis. Their color was white in 28°C mice and brownish (i.e., paler than the anterior subcutaneous depot) in 6°C mice (Fig. 1).

Visceral fat. All visceral depots (see supplementary Table I for nomenclature) found in the abdomen were in contact with the peritoneum. Some (mesenteric, interrenal, periovarian, parametrial, and perivesical) lay between two visceral peritoneal sheets (i.e., in the peritoneal ligaments); others lay behind the parietal peritoneum–retroperitoneal depot.

We have denominated the dissectible, single but complex depot formed by the interrenal, periovarian, parametrial, and perivesical subdepots the “abdominopelvic depot.” This depot surrounds the kidneys and ovaries in the abdomen and extends to the pelvis, where it is sheathed by the peritoneal folds of the uterus (parametrium) and surrounds the bladder.

The thoracic depot was found in the mediastinum, surrounding the heart, the aorta, and its main collaterals. Of note, the mediastinal depot was continuous (through the aortic hiatus) with the abdominopelvic depot, where the fat surrounding the aorta was continuous with the interrenal fat. Interestingly, histological examination documented a transition from the tissue lying near the aorta and the roots of its main collaterals, which was predominantly composed of BAT, to the rest of the mediastinal and abdominopelvic depots, which were essentially made up of WAT (Fig. 2). Of the visceral fat depots, only the mediastinal was brownish in 28°C mice. In 6°C mice, there were some brownish areas in the interrenal, periovarian, and parametrial portions of the abdominopelvic depot, whereas the mediastinal depot was dark brown (the brownest part in the whole adipose organ).

The retroperitoneal depot had a typical elongated, conical shape and occupied the grooves on the sides of the psoas muscles, behind the peritoneum. After cold acclimation, its white color turned a pale brown hue (Fig. 1).

TABLE 1. Adipose organ composition and parenchymal nerve fiber density in C57BL/6J obesity-prone mice

	Anterior Subcutaneous	Posterior Subcutaneous	Mediastinal	Mesenteric	Retroperitoneal	Abdominopelvic
C57BL/6J						
No. unilocular adipocytes						
28°C	56 ± 8 ^{###}	14 ± 1	6 ± 3 ^{##}	12 ± 1	2 ± 1	27 ± 2
6°C	25 ± 5 ^{*##}	16 ± 3	0.6 ± 0.3	10 ± 1 [#]	2 ± 0.2	15 ± 4*
No. UCPI-negative multilocular adipocytes						
28°C	8 ± 0.3 [#]	1 ± 0.2	0.2 ± 0.08 [#]	0.7 ± 0.4	0	5 ± 0.8 [#]
6°C	6 ± 1 ^{##}	2 ± 0.4*	3 ± 0.1 [#]	1 ± 0.3 [#]	0.4 ± 0.1	11 ± 0.8
No. UCPI-positive multilocular adipocytes						
28°C	12 ± 4 ^{###}	0	8 ± 3	0	0	0.7 ± 0.4
6°C	54 ± 4 ^{*##}	0.6 ± 0.2 ^{##}	7 ± 1	0.03 ± 0.002	0.001 ± 0.0002	7 ± 2 [#]
TH-positive fiber density						
28°C	11 ± 2	2 ± 0.8	34 ± 0.7 ^{###}	6 ± 2 ^{###}	2 ± 1	16 ± 1
6°C	61 ± 5 ^{*##}	6 ± 2 ^{##}	50 ± 9	9 ± 2 ^{###}	7 ± 2	31 ± 3*
SV129						
No. unilocular adipocytes						
28°C	16 ± 3	19 ± 0.2	0.1 ± 0.1	10 ± 0.8	2 ± 0.5	22 ± 1
6°C	9 ± 2*	16 ± 1*	0	4 ± 2 ^{**}	2 ± 0.6	9 ± 1 ^{***}
No. UCPI-negative multilocular adipocytes						
28°C	2 ± 0.3	0.9 ± 0.5	0.05 ± 0.03	0	0.1 ± 0.1	9 ± 2
6°C	11 ± 3*	4 ± 1*	0.1 ± 0.04	10 ± 2 ^{**}	0.1 ± 0	7 ± 1
No. UCPI-positive multilocular adipocytes						
28°C	73 ± 6	0	5 ± 1	0	0.006 ± 0.006	15 ± 3
6°C	73 ± 5	6 ± 1 ^{***}	9 ± 2	0.2 ± 0.03*	0.4 ± 0.1 ^{**}	25 ± 3*
TH-positive fiber density						
28°C	12 ± 7	1 ± 0.2	78 ± 2	1 ± 0.1	0.2 ± 0.1	16 ± 2
6°C	45 ± 8*	12 ± 2 ^{**}	72 ± 26	20 ± 2 ^{**}	2 ± 0.9	38 ± 0.8 ^{**}

Data of obesity-resistant Sv129 mice from a previous work (26) are provided for comparison. Number of adipocytes × 10⁶. TH-positive fibers/100 adipocytes.

^{*}Indicates statistically significant difference between temperature conditions (same depot, same strain). *P < 0.05; **P < 0.01; ***P < 0.001.

[#]Indicates statistically significant difference between strains (same depot, same temperature condition). #P < 0.05; ##P < 0.01; ###P < 0.001.

Total number of adipocytes contained in the adipose organ of C57BL/6J and Sv129 results unchanged. P = 0.25 in 28°C mice; P = 0.18 in 6°C mice.

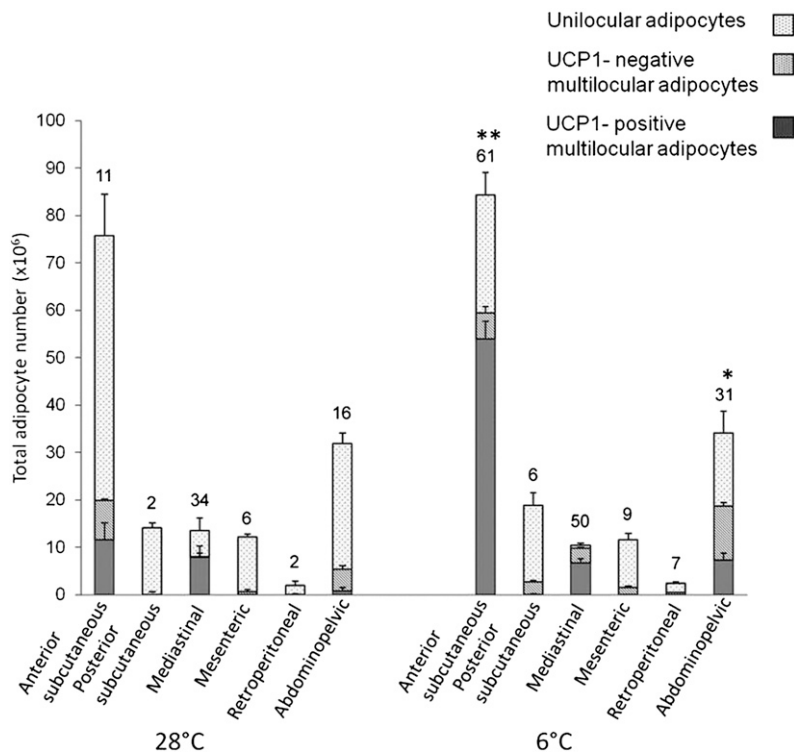


Fig. 4. Number of unilocular, UCP1-negative multilocular and UCP1-positive multilocular adipocytes in different depots of the adipose organ of C57BL/6J mice maintained at 28°C or 6°C for 10 days. In the cold-acclimated group, the number of UCP1-positive multilocular adipocytes increased significantly in the anterior subcutaneous and in the abdominopelvic depot. Numbers above columns indicate the average density of TH-positive parenchymal fibers in each depot (fiber number/100 adipocytes). Data are mean \pm SEM. * $P < 0.05$, ** $P < 0.01$.

Quantitative histology and immunohistochemistry

Morphology and immunohistochemistry for the protein marker of brown adipocytes, UCP1, allowed three types of adipocytes to be distinguished in the fat depots: UCP1-positive multilocular adipocytes (usually described as brown adipocytes), UCP1-negative unilocular adipocytes (commonly described as white adipocytes), and UCP1-negative multilocular adipocytes (**Fig. 3A**). White adipocytes aggregated into WAT and brown adipocytes into BAT. UCP1-negative multilocular adipocytes had slightly different morphological features compared with brown adipocytes (i.e., UCP1-positive multilocular adipocytes), especially the lipid droplets, which were larger (+37% in 28°C mice and +75% in 6°C mice) and fewer (≤ 10 /cell versus > 10 /cell) than those of brown adipocytes ($P = 0.01$ in 28°C mice and $P < 0.0001$ in 6°C mice). These adipocytes were mainly found in transition areas between BAT and WAT.

Our quantitative measurements show that white adipocytes were the predominant cell type in the adipose organ of 28°C mice, whereas brown adipocytes became the prevalent cell type in 6°C mice (**Fig. 3B**). Of note, this change in cell composition occurred in the absence of any significant change in total adipocyte count ($150 \pm 17 \times 10^6$ versus $161 \pm 8 \times 10^6$; $P = 0.6$) or in the number of UCP1-negative multilocular adipocytes ($17 \pm 3 \times 10^6$ versus $19 \pm 2 \times 10^6$; $P = 0.5$) in the organ; i.e., the increase in the number of brown adipocytes ($+55 \times 10^6 \pm 7$; $P < 0.001$) nearly equaled the decrease in the number of white adipocytes ($-47 \times 10^6 \pm 9$; $P = 0.05$) (**Fig. 3B**). The only exception was the interscapular part of the anterior subcutaneous depot (widely held to be the classic interscapular BAT), where the adipocyte number increased ($P = 0.07$), albeit not significantly,

in cold-acclimated mice (supplementary Table II). We noted no signs of apoptosis (31) or degeneration of white adipocytes or mitotic figures in any of the slides examined (66 sections/mouse, 1000 \times final magnification).

In 6°C mice, the number of multilocular adipocytes increased in all depots as did the proportion of UCP1-positive multilocular adipocytes, from $50 \pm 3\%$ of all multilocular adipocytes in 28°C mice to $78 \pm 1\%$ of all multilocular adipocytes in 6°C mice ($P < 0.01$), leaving the proportion of UCP1-negative multilocular adipocytes unchanged ($12 \pm 3\%$ in 28°C mice versus $9 \pm 1\%$ in 6°C mice; $P = 0.86$). With regard to the depots, it should be emphasized that all had a mixed tissue composition (white, brown, and UCP1-negative multilocular adipocytes, or at least, white and UCP1-negative multilocular cells) in both experimental conditions, with the exception of the small retroperitoneal depot, where only white adipocytes were found in 28°C mice. In cold-acclimated mice, brown adipocytes were found in all depots (**Table 1**). Their increase was significant in the anterior subcutaneous ($P < 0.001$) and abdominopelvic depots ($P = 0.03$) (**Fig. 4**) and, interestingly, in nearly all of their areas (**Fig. 5**). Of note, in 28°C mice, UCP1 immunoreactivity in brown adipocytes was weaker and the lipid droplets were fewer (< 10 /cell at 28°C versus > 15 /cell at 6°C) and larger (+67%) in all depots compared with 6°C mice (supplementary Fig. 1).

The volume of the adipose organ as a whole, calculated by measuring fluid displacement (see Materials and Methods) was reduced in 6°C mice ($2,201 \pm 127$ versus $1,637 \pm 129 \mu\text{l}$; $P = 0.05$). The reduction involved each depot (see **Table 2**) and was ascribed to adipocyte shrinking (unilocular adipocytes: $22,617 \pm 993$ versus $16,471 \pm 245 \mu\text{m}^3 \times 10^9$, $P = 0.02$; multilocular adipocytes: $6,900 \pm 335$ versus

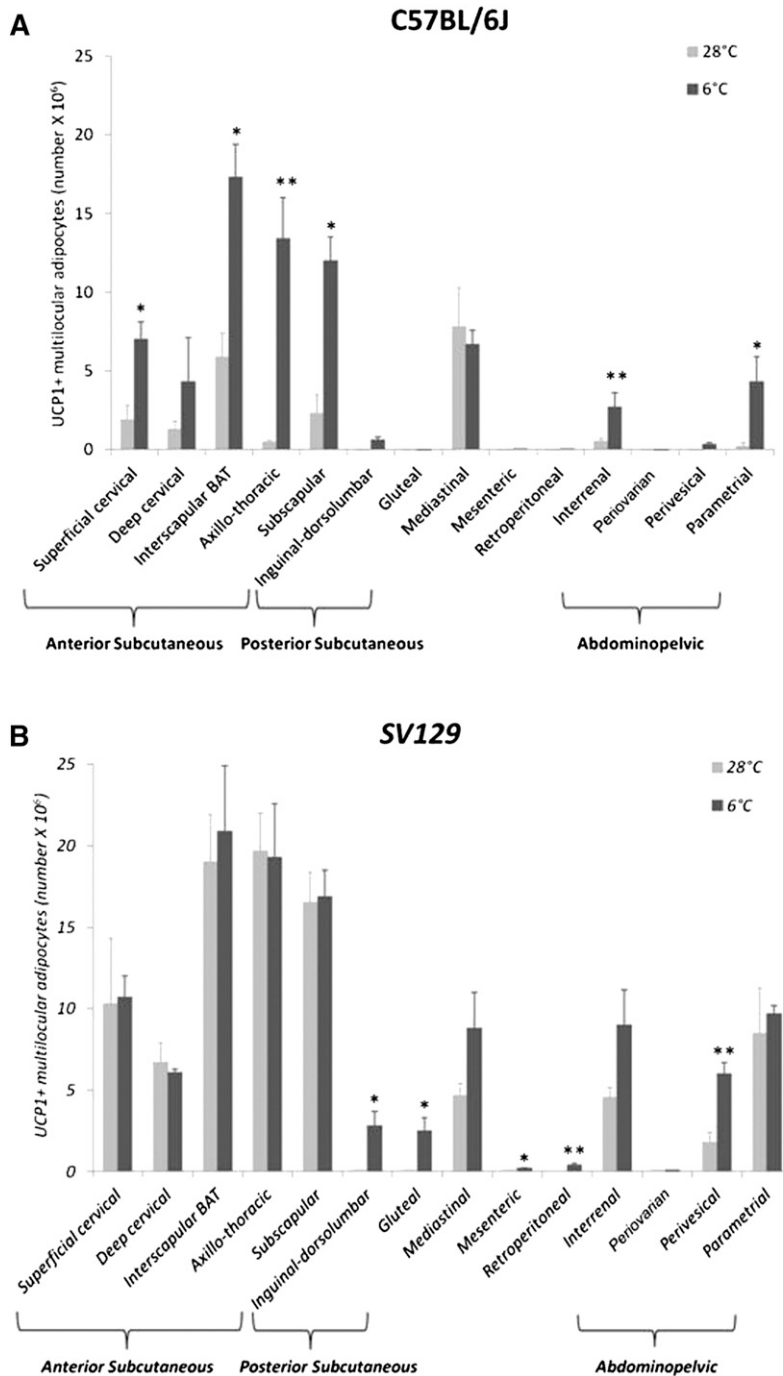


Fig. 5. Number of UCP1-positive multilocular adipocytes at 28°C and after cold exposure. (A) C57BL/6J and (B) Sv129 mice: anterior subcutaneous depot (composed of superficial cervical, deep cervical, interscapular, axillo-thoracic, and subscapular portions); posterior subcutaneous depot (composed of inguinal-dorsolumbar and gluteal portions); mediastinal depot, mesenteric depot, retroperitoneal depot, and abdominopelvic depot (composed of interrenal, periovarian, perivesical, parametrial, and periovarian portions). The data on C57BL/6J mice are the same presented in supplementary Table II. Sv129 data were obtained from a previous work (26). Mean ± SEM. * $P < 0.05$, ** $P < 0.01$.

$6,723 \pm 545 \mu\text{m}^3 \times 10^9$, $P = 0.5$) (supplementary Fig. II). In fact, when the volume reduction of each multilocular and unilocular adipocyte was multiplied by the number of these cells, it equaled the overall volume reduction seen in 6°C mice.

Parenchymal innervation

The prevalent type of parenchymal nerve fiber in adipose tissue is noradrenergic (1–37); TH immunoreactivity is widely considered as a marker of noradrenergic fibers (38).

We observed and counted the TH-positive parenchymal fibers in contact with adipocytes in all depots (and ignored the TH-positive fibers associated with larger vessels and

nerves) in both experimental conditions. TH-positive fibers were detected in areas containing unilocular adipocytes as well as in areas containing multilocular adipocytes, but they were densest in the latter areas, especially where multilocular adipocytes had smaller and more numerous lipid droplets, i.e., in cells whose morphology resembled that of UCP1-positive multilocular adipocytes (Fig. 6A–C). To avoid any bias due to adipocyte shrinking at 6°C, the density of TH-positive fibers was measured as fiber number/100 adipocytes.

In the whole adipose organ, the density of TH-positive fibers increased about 2.3 times after cold acclimation ($P = 0.004$) (Fig. 6D). Their density increased in all depots in 6°C mice (Table 1), and the change was significant in

TABLE 2. Volume of adipose depots of C57BL/6J mice kept at 28°C or 6°C for 10 days

		Subcutaneous	Mediastinal	Mesenteric	Retroperitoneal	Abdominopelvic	Total
28°C	1	1,605	100	250	50	580	2,585
	2	1,290	120	300	24	570	2,304
	3	1,160	120	300	160	520	2,165
	4	1,240	120	200	43	550	2,153
	5	1,043	80	190	30	445	1,798
Mean ± SEM		1,268 ± 93	108 ± 8	228 ± 21	61 ± 25	535 ± 22	2,201 ± 127
6°C	1	920	60	100	40	425	1,545
	2	955	60	120	50	410	1,595
	3	1,017	110	150	60	410	1,747
	4	860	100	100	40	378	1,478
	5	1,040	100	180	40	460	1,820
Mean ± SEM		958 ± 70 <i>P</i> = 0.05	86 ± 11 <i>P</i> = 0.18	130 ± 24 <i>P</i> = 0.023	46 ± 4 <i>P</i> = 0.6	416 ± 26 <i>P</i> = 0.03	1,637 ± 129 <i>P</i> = 0.05

Volume in microliters.

those depots exhibiting a significant increase in UCP1-positive multilocular adipocytes, i.e., anterior subcutaneous ($P = 0.008$) and abdominopelvic ($P = 0.001$) depots (Fig. 4). A positive correlation between density of TH-positive fibers and density of UCP1-positive multilocular adipocytes was found in both experimental conditions and in both mouse strains (C57BL/6J here and Sv129 previously), but it was stronger in 6°C than in 28°C mice (Fig. 7).

DISCUSSION

The adipose organ of C57BL/6J mice has a mixed composition

Our gross anatomy data show that most of the dissectible fat of warm- and cold-acclimated C57BL/6J mice is contained in visceral and subcutaneous depots, whose shape is comparable to those found in other strains (26, 27). Morphology and UCP1 staining demonstrated that most depots are composed of three specific types of adipocytes: UCP1-negative unilocular (usually described as white) adipocytes, UCP1-positive multilocular (usually described as brown) adipocytes, and UCP1-negative multilocular adipocytes. The latter cells have also been described (by our group) in interscapular BAT after acute adrenergic stimulation as part of a phenomenon designated as the Harlequin effect (34). However, the UCP1-negative multilocular adipocytes of the Harlequin effect are identical to and intermingled with UCP1-positive multilocular adipocytes, whereas those described here have a different morphology (fewer and larger lipid droplets) and are mainly found in border areas between WAT and BAT; a further difference is that large amounts of the former are also found in fat depots of warm-acclimated mice. Thus the UCP1-negative multilocular adipocytes described here appear to be different from those of the Harlequin effect and could be intermediate forms between white and brown adipocytes, in line with findings presented recently by our group (7). Therefore, C57BL/6J mice have a multidepot organ predominantly composed of a mixed population of adipocytes. These data confirm

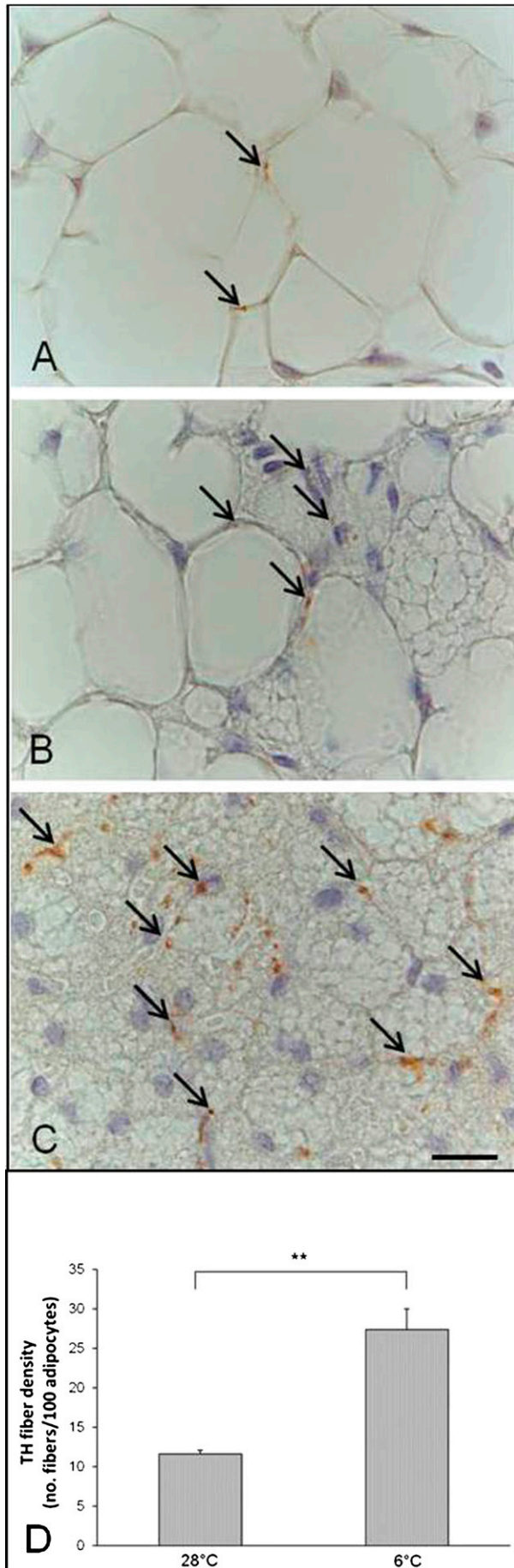
in C57BL/6J mice our earlier results obtained in the Sv129 adipose organ (26, 27).

Plasticity of the adipose organ

The presence of areas formed by a mixture of white adipocytes, UCP1-negative multilocular adipocytes, and brown adipocytes can probably be ascribed to the high plasticity of the adipose organ, where cold acclimation induces a tissue composition change involving an increase in brown adipocytes (and a corresponding decrease in white adipocytes) in many depots, without significant changes in the total number of adipocytes in the organ. This finding, together with data published by our laboratory as well as others (7, 8), suggests that at least part of the newly formed brown adipocytes may arise as a result of the direct transformation of white into brown adipocytes.

In this regard, three different groups using different methods have reached the conclusion that the cells in “classical BAT depots (interscapular BAT)” are ontogenically different from brown adipocytes arising in WAT depots (39–41). The data obtained here confirm the unique behavior of interscapular BAT, the only subdepot where the brown adipocyte increase cannot be explained by direct transformation of pre-existing cells. Thus, the arising of new brown adipocytes after cold exposure and acclimation is consistent with the hypothesis of their origin from preadipocyte proliferation (where interscapular BAT is concerned) and from white to brown transdifferentiation (in the other depots), as also reported in a recent work by our group (7).

The simultaneous presence of white and brown adipocytes in fat depots of mice not subjected to adrenergic stimulation raises the question of its rationale, given the opposite functions of the two cells (white adipocytes store lipids, brown adipocytes burn them), especially if UCP1-negative multilocular adipocytes are considered as intermediate stages in the transformation of white into brown adipocytes (7). To answer this question, we advanced the theory of reversible transdifferentiation; i.e., that chronic cold exposure makes white adipocytes turn into brown adipocytes to enhance heat production, whereas exposure to an obesogenic environment turns brown adipocytes into white adipocytes



to increase energy storage capacity (42). MRI and histological studies in rats have documented the plasticity of interscapular BAT, suggesting the reversibility of this phenomenon (43, 44). Such tissue plasticity does not seem to be confined to these types of stimuli, as mammary gland adipocytes are able to transform reversibly into milk-secreting glands during pregnancy and lactation (45, 46).

Nerve fiber plasticity

Browning of the adipose organ after cold exposure is blunted in $\beta 3$ knockout mice both in C57BL/6J and Sv129 animals (7–47). Noradrenaline, the major molecular factor acting on $\beta 3$ adrenoceptors, is secreted by noradrenergic fibers (1). These can be identified using anti-TH antibody. The number of TH-positive parenchymal fibers per 100 adipocytes (in direct contact with them) was greater in the adipose organ of Sv129 than C57BL/6J mice. Their density in C57BL/6J mice increased significantly after cold acclimation (by 2.3 times). Of note, in the same experimental condition, TH-positive parenchymal fibers also increased significantly in Sv129 mice, but only by 1.7 times, suggesting a more plastic SNS response in C57BL/6J mice or a “ceiling effect” in the Sv129 mice due to the large amount of BAT already present in this strain. Thus, it was not surprising to find a positive correlation between density of TH-positive parenchymal fibers and number of brown adipocytes in C57BL/6J mice, too. Notably, the density of TH-positive fibers in the latter strain was minimal in areas composed of unilocular adipocytes, maximal in areas composed of classic multilocular adipocytes with small lipid droplets, and intermediate in areas composed of multilocular adipocytes with large lipid droplets; i.e., the density of noradrenergic fibers was related to adipocyte morphology. Altogether, these data suggest that the different susceptibility of C57BL/6J and Sv129 mice to obesity and type 2 diabetes could be due to the genetically determined parenchymal innervation of the adipose organ, involving different numbers of brown adipocytes in the two strains.

In fact, given that brown adipocytes produce neuroattractant (48–50) as well as neurorepellant (51) factors, the reverse mechanism (i.e., genetically determined brown adipocyte numbers involving different nerve fiber density) cannot be excluded. However, cold exposure seems to activate primarily the central nervous system (52), making the browning phenomenon more likely to be secondary, also in relation to the scarce number of brown adipocytes detected at 28°C and to the high reactivity of TH-positive parenchymal fibers after cold exposure in C57BL/6J mice. Branching of TH-positive parenchymal fiber is found in both strains but is greater in C57BL/6J mice, suggesting

Fig. 6. TH-positive (brown) parenchymal nerve fibers in three different areas of the adipose organ of C57BL/6J mice: (A) unilocular area, (B) mixed area, and (C) multilocular area. Arrows indicate some TH-positive parenchymal nerve fibers. Scale bar: 15 μ m for all. (D) Mean density of TH-positive parenchymal nerve fibers in the whole adipose organ of 28°C or 6°C mice. Data are shown as mean \pm SEM. ** $P < 0.01$.

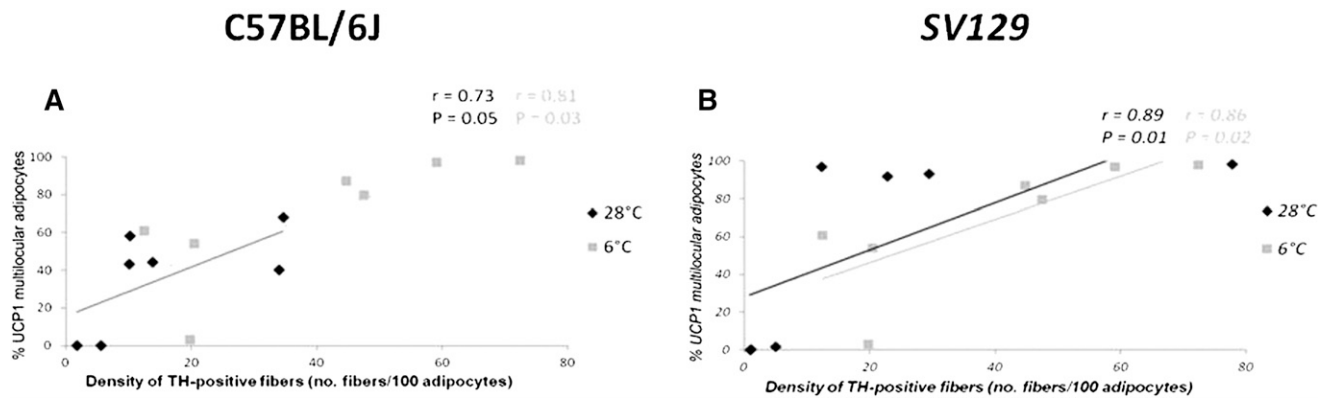


Fig. 7. Correlation between density of TH-positive parenchymal fibers and proportion of UCP1-positive multilocular adipocytes in different adipose depots of C57BL/6J (A) and Sv129 (B) mice maintained at 28°C or 6°C for 10 days. Sv129 data from a previous work (26) are in italics. Linear correlations were calculated using Spearman's nonparametric test; r = Spearman coefficient; P = probability.

that mammals with a limited BAT could also be selected for browning therapeutic strategies. This is especially important given the recent demonstration of metabolically active BAT (14–17) provided with TH-positive parenchymal nerves in normal adult humans (18).

Comparison of data from Sv129 and C57BL/6J mice

Comparison with data from previous works (26, 27) shows that the adipose organ of obesity-resistant Sv129 mice and obesity-prone C57BL/6J mice contains similar amounts of adipocytes (Table 1) but differs in a major characteristic: the number of brown adipocytes at 28°C. In fact, these account for about 53% of all adipocytes in Sv129 mice (26, 27) and for about 14% in C57BL/6J mice. Cold exposure for 10 days resulted in a smaller and browner adipose organ in both strains: the adipocytes shrank, and multiplication of their mean volume loss by their number was found to equal the overall volume reduction measured in cold-acclimated mice. It should also be noted that the increase in brown adipocytes seen in C57BL/6J mice (+350%) after cold exposure was much larger than that observed in Sv129 mice (+30%). These data are in line with the genetic variability of the adipocyte composition of fat depots and of the reaction to adrenergic stimuli found in different strains (23, 24).

The periovarian, parametrial, and interrenal fat depots are usually described as separate entities. We demonstrated in Sv129 mice (26, 27) and confirmed here in C57BL/6J mice that they are, in fact, parts of a single, well-defined depot extending from the abdomen to the pelvis. For this reason and as proposed previously (26), we feel that it should be called the abdominopelvic depot. Here we show that it is continuous with the mediastinal depot through the aortic hiatus, suggesting that both are more closely related to the aorta and its main collaterals than to their respective anatomical districts. These topographical features suggest that the rationale of the close association of the brown component of the two depots to the aorta and its main branches could be facilitation of heat transfer to the rest of the organism. Indeed, the histological data documented a transition from deeply brown fat in the vicinity of the aorta to a whiter morphology in the farthest part of the two depots.

In conclusion, our data support the notion of the adipose organ and highlight a different brown adipocyte component in obesity-resistant (Sv129) and obesity-prone (C57BL/6J) strains. Harnessing the strong browning response to cold exposure of the C57BL/6J adipose organ is a promising approach to developing therapeutic strategies to curb obesity and type 2 diabetes in patients with constitutively low amounts of BAT (28–54). **EM**

REFERENCES

- Cannon, B., and J. Nedergaard. 2004. Brown adipose tissue: function and physiological significance. *Physiol. Rev.* **84**: 277–359.
- Cinti, S. 2002. Adipocyte differentiation and transdifferentiation: plasticity of the adipose organ. *J. Endocrinol. Invest.* **25**: 823–835.
- Cinti, S. 2005. The adipose organ. *Prostaglandins Leukot. Essent. Fatty Acids.* **73**: 9–15.
- Cinti, S. 1999. *The Adipose Organ*. Editrice Kurtis, Milan.
- Frontini, A., and S. Cinti. 2010. Distribution and development of brown adipocytes in the murine and human adipose organ. *Cell Metab.* **11**: 253–256.
- Himms-Hagen, J., A. Melnyk, M. C. Zingaretti, E. Ceresi, G. Barbatelli, and S. Cinti. 2000. Multilocular fat cells in WAT of CL-316243-treated rats derive directly from white adipocytes. *Am. J. Physiol. Cell Physiol.* **279**: C670–C681.
- Barbatelli, G., I. Murano, L. Madsen, Q. Hao, M. Jimenez, K. Kristiansen, J. P. Giacobino, R. De Matteis, and S. Cinti. 2010. The emergence of cold-induced brown adipocytes in mouse white fat depots is determined predominantly by white to brown adipocyte transdifferentiation. *Am. J. Physiol. Endocrinol. Metab.* **298**: E1244–E1253.
- Granneman, J. G., P. Li, Z. Zhu, and Y. Lu. 2005. Metabolic and cellular plasticity in white adipose tissue I: effects of beta3-adrenergic receptor activation. *Am. J. Physiol. Endocrinol. Metab.* **289**: E608–E616.
- Lowell, B. B., V. S. Susulic, A. Hamann, J. A. Lawitts, J. Himms-Hagen, B. B. Boyer, L. P. Kozak, and J. S. Flier. 1993. Development of obesity in transgenic mice after genetic ablation of brown adipose tissue. *Nature.* **366**: 740–742.
- Bachman, E. S., H. Dhillon, C. Y. Zhang, S. Cinti, A. C. Bianco, B. K. Kobilka, and B. B. Lowell. 2002. betaAR signaling required for diet-induced thermogenesis and obesity resistance. *Science.* **297**: 843–845.
- Kopecky, J., G. Clarke, S. Enerback, B. Spiegelman, and L. P. Kozak. 1995. Expression of the mitochondrial uncoupling protein gene from the aP2 gene promoter prevents genetic obesity. *J. Clin. Invest.* **96**: 2914–2923.
- Ghorbani, M., and J. Himms-Hagen. 1997. Appearance of brown adipocytes in white adipose tissue during CL 316,243-induced reversal of obesity and diabetes in Zucker fa/fa rats. *Int. J. Obes. Relat. Metab. Disord.* **21**: 465–475.
- Ghorbani, M., and J. Himms-Hagen. 1998. Treatment with CL 316,243, a beta 3-adrenoceptor agonist, reduces serum leptin in rats

- with diet- or aging-associated obesity, but not in Zucker rats with genetic (fa/fa) obesity. *Int. J. Obes. Relat. Metab. Disord.* **22**: 63–65.
14. Cypess, A. M., S. Lehman, G. Williams, I. Tal, D. Rodman, A. B. Goldfine, F. C. Kuo, E. L. Palmer, Y. H. Tseng, A. Doria, et al. 2009. Identification and importance of brown adipose tissue in adult humans. *N. Engl. J. Med.* **360**: 1509–1517.
 15. Saito, M., Y. Okamatsu-Ogura, M. Matsushita, K. Watanabe, T. Yoneshiro, J. Nio-Kobayashi, T. Iwanaga, M. Miyagawa, T. Kameya, K. Nakada, et al. 2009. High incidence of metabolically active brown adipose tissue in healthy adult humans: effects of cold exposure and adiposity. *Diabetes.* **58**: 1526–1531.
 16. van Marken Lichtenbelt, W. D., J. W. Vanhommerig, N. M. Smulders, J. M. Drossaerts, G. J. Kemerink, N. D. Bouvy, P. Schrauwen, and G. J. Teule. 2009. Cold-activated brown adipose tissue in healthy men. *N. Engl. J. Med.* **360**: 1500–1508.
 17. Virtanen, K. A., M. E. Lidell, J. Orava, M. Heglund, R. Westergren, T. Niemi, M. Taittonen, J. Laine, N. J. Savisto, S. Enerback, et al. 2009. Functional brown adipose tissue in healthy adults. *N. Engl. J. Med.* **360**: 1518–1525.
 18. Zingaretti, M. C., F. Crosta, A. Vitali, M. Guerrieri, A. Frontini, B. Cannon, J. Nedergaard, and S. Cinti. 2009. The presence of UCPI1 demonstrates that metabolically active adipose tissue in the neck of adult humans truly represents brown adipose tissue. *FASEB J.* **23**: 3113–3120.
 19. Cohade, C., M. Osman, H. K. Pannu, and R. L. Wahl. 2003. Uptake in supraclavicular area fat (“USA-Fat”): description on 18F-FDG PET/CT. *J. Nucl. Med.* **44**: 170–176.
 20. Nedergaard, J., T. Bengtsson, and B. Cannon. 2007. Unexpected evidence for active brown adipose tissue in adult humans. *Am. J. Physiol. Endocrinol. Metab.* **293**: E444–E452.
 21. Almind, K., and C. R. Kahn. 2004. Genetic determinants of energy expenditure and insulin resistance in diet-induced obesity in mice. *Diabetes.* **53**: 3274–3285.
 22. Surwit, R. S., M. N. Feinglos, J. Rodin, A. Sutherland, A. E. Petro, E. C. Opara, C. M. Kuhn, and M. Rebuffe-Scrive. 1995. Differential effects of fat and sucrose on the development of obesity and diabetes in C57BL/6J and A/J mice. *Metabolism.* **44**: 645–651.
 23. Guerra, C., R. A. Koza, H. Yamashita, K. Walsh, and L. P. Kozak. 1998. Emergence of brown adipocytes in white fat in mice is under genetic control. Effects on body weight and adiposity. *J. Clin. Invest.* **102**: 412–420.
 24. Collins, S., K. W. Daniel, A. E. Petro, and R. S. Surwit. 1997. Strain-specific response to beta 3-adrenergic receptor agonist treatment of diet-induced obesity in mice. *Endocrinology.* **138**: 405–413.
 25. Almind, K., M. Manieri, W. I. Sivitz, S. Cinti, and C. R. Kahn. 2007. Ectopic brown adipose tissue in muscle provides a mechanism for differences in risk of metabolic syndrome in mice. *Proc. Natl. Acad. Sci. USA.* **104**: 2366–2371.
 26. Murano, I., G. Barbatelli, A. Giordano, and S. Cinti. 2009. Noradrenergic parenchymal nerve fiber branching after cold acclimatization correlates with brown adipocyte density in mouse adipose organ. *J. Anat.* **214**: 171–178.
 27. Murano, I., C. M. Zingaretti, and S. Cinti. 2005. The adipose organ of Sv129 mice contains a prevalence of brown adipocytes and shows plasticity after cold exposure. *Adipocytes.* **1**: 121–130.
 28. Cypess, A. M., and C. R. Kahn. 2010. Brown fat as a therapy for obesity and diabetes. *Curr. Opin. Endocrinol. Diabetes Obes.* **17**: 143–149.
 29. Giordano, A., A. Frontini, and S. Cinti. 2008. Adipose organ nerves revealed by immunohistochemistry. *Methods Mol. Biol.* **456**: 83–95.
 30. Himms-Hagen, J. 1986. Brown adipose tissue and cold-acclimation. In *Brown Adipose Tissue*. P. Trayhurn and D. Nicholls. Edward Arnold, London. 214–268.
 31. Kerr, J. F., C. M. Winterford, and B. V. Harmon. 1994. Morphological criteria for identifying apoptosis. In *Cell Biology: A Laboratory Handbook*. J. E. Celis, editor. Academic Press, San Diego. 319–329.
 32. Hsu, S. M., L. Raine, and H. Fanger. 1981. Use of avidin-biotin-peroxidase complex (ABC) in immunoperoxidase techniques: a comparison between ABC and unlabeled antibody (PAP) procedures. *J. Histochem. Cytochem.* **29**: 577–580.
 33. De Matteis, R., D. Ricquier, and S. Cinti. 1998. TH-, NPY-, SP-, and CGRP-immunoreactive nerves in interscapular brown adipose tissue of adult rats acclimated at different temperatures: an immunohistochemical study. *J. Neurocytol.* **27**: 877–886.
 34. Cinti, S., R. Cancelli, M. C. Zingaretti, E. Ceresi, R. De Matteis, A. Giordano, J. Himms-Hagen, and D. Ricquier. 2002. CL316,243 and cold stress induce heterogeneous expression of UCPI1 mRNA and protein in rodent brown adipocytes. *J. Histochem. Cytochem.* **50**: 21–31.
 35. Weibel, E. R., editor. 1980. *Stereological Methods: Practical Methods for Biological Morphometry*. Vol. 1. Academic Press, London.
 36. Giordano, A., M. Morroni, G. Santone, G. F. Marchesi, and S. Cinti. 1996. Tyrosine hydroxylase, neuropeptide Y, substance P, calcitonin gene-related peptide and vasoactive intestinal peptide in nerves of rat periovarian adipose tissue: an immunohistochemical and ultrastructural investigation. *J. Neurocytol.* **25**: 125–136.
 37. Giordano, A., M. Morroni, F. Carle, R. Gesuita, G. F. Marchesi, and S. Cinti. 1998. Sensory nerves affect the recruitment and differentiation of rat periovarian brown adipocytes during cold acclimation. *J. Cell Sci.* **111**: 2587–2594.
 38. Bartness, T. J., and C. K. Song. 2007. Thematic review series: adipocyte biology. Sympathetic and sensory innervation of white adipose tissue. *J. Lipid Res.* **48**: 1655–1672.
 39. Seale, P., B. Bjork, W. Yang, S. Kajimura, S. Chin, S. Kuang, A. Scime, S. Devarakonda, H. M. Conroe, H. Erdjument-Bromage, et al. 2008. PRDM16 controls a brown fat/skeletal muscle switch. *Nature.* **454**: 961–967.
 40. Petrovic, N., T. B. Walden, I. G. Shabalina, J. A. Timmons, B. Cannon, and J. Nedergaard. 2010. Chronic peroxisome proliferator-activated receptor gamma (PPARgamma) activation of epididymally derived white adipocyte cultures reveals a population of thermogenically competent, UCPI1-containing adipocytes molecularly distinct from classic brown adipocytes. *J. Biol. Chem.* **285**: 7153–7164.
 41. Atit, R., S. K. Sgaier, O. A. Mohamed, M. M. Taketo, D. Dufort, A. L. Joyner, L. Niswander, and R. A. Conlon. 2006. Beta-catenin activation is necessary and sufficient to specify the dorsal dermal fate in the mouse. *Dev. Biol.* **296**: 164–176.
 42. Cinti, S. 2009. Transdifferentiation properties of adipocytes in the adipose organ. *Am. J. Physiol. Endocrinol. Metab.* **297**: E977–E986.
 43. Sbarbati, A., A. M. Baldassarri, C. Zancanaro, A. Boicelli, and F. Osculati. 1991. In vivo morphology and functional morphology of brown adipose tissue by magnetic resonance imaging. *Anat. Rec.* **231**: 293–297.
 44. Osculati, F., F. Leclercq, A. Sbarbati, C. Zancanaro, S. Cinti, and K. Antonakis. 1989. Morphological identification of brown adipose tissue by magnetic resonance imaging in the rat. *Eur. J. Radiol.* **9**: 112–114.
 45. De Matteis, R., M. C. Zingaretti, I. Murano, A. Vitali, A. Frontini, I. Giannulusi, G. Barbatelli, F. Marcucci, M. Bordicchia, R. Sarzani, et al. 2009. In vivo physiologic transdifferentiation of adult adipose cells. *Stem Cells.* **27**: 2761–2768.
 46. Morroni, M., R. De Matteis, C. Palumbo, M. Ferretti, I. Villa, A. Rubinacci, S. Cinti, and G. Marotti. 2004. In vivo leptin expression in cartilage and bone cells of growing rats and adult humans. *J. Anat.* **205**: 291–296.
 47. Jimenez, M., G. Barbatelli, R. Allevi, S. Cinti, J. Seydoux, J. P. Giacobino, P. Muzzin, and F. Preitner. 2003. Beta 3-adrenoceptor knockout in C57BL/6J mice depresses the occurrence of brown adipocytes in white fat. *Eur. J. Biochem.* **270**: 699–705.
 48. Nisoli, E., C. Tonello, M. Benarese, P. Liberini, and M. O. Carruba. 1996. Expression of nerve growth factor in brown adipose tissue: implications for thermogenesis and obesity. *Endocrinology.* **137**: 495–503.
 49. Nisoli, E., C. Tonello, and M. O. Carruba. 1998. Nerve growth factor, beta3-adrenoceptor and uncoupling protein 1 expression in rat brown fat during postnatal development. *Neurosci. Lett.* **246**: 5–8.
 50. Néchad, M., E. Ruka, and J. Thibault. 1994. Production of nerve growth factor by brown fat in culture: relation with the in vivo developmental stage of the tissue. *Comp. Biochem. Physiol. Comp. Physiol.* **107**: 381–388.
 51. Giordano, A., R. Coppari, M. Castellucci, and S. Cinti. 2001. Sema3a is produced by brown adipocytes and its secretion is reduced following cold acclimation. *J. Neurocytol.* **30**: 5–10.
 52. Nautiyal, K. M., M. Dailey, N. Brito, M. N. Brito, R. B. Harris, T. J. Bartness, and H. J. Grill. 2008. Energetic responses to cold temperatures in rats lacking forebrain-caudal brain stem connections. *Am. J. Physiol. Regul. Integr. Comp. Physiol.* **295**: R789–R798.
 53. Bartelt, A., O. T. Bruns, R. Reimer, H. Hohenberg, H. Itrich, K. Peldschus, M. G. Kaul, U. I. Tromsdorf, H. Weller, C. Waurisch, et al. 2011. Brown adipose tissue activity controls triglyceride clearance. *Nat. Med.* **17**: 200–205.
 54. Nedergaard, J., T. Bengtsson, and B. Cannon. 2010. Three years with adult human brown adipose tissue. *Ann. N. Y. Acad. Sci.* **1212**: E20–E36.